

Passive Radio Frequency Identification Tag with Frequency Doubler and Energy Harvesting

Alina-Cristina BUNEA¹, Ovidiu George PROFIRESCU², and
Dan NECULOIU^{1, 2, *}

¹National Institute of R&D in Microtechnologies (IMT) Bucharest, 077190, Romania

²National University for Science and Technology POLITEHNICA Bucharest, 060042, Romania

E-mails: alina.bunea@imt.ro, dan.neculoiu@imt.ro*

* Corresponding author

Abstract. The paper presents the simulation and experimental results obtained for a passive RFID tag based on the integration of microstrip patch antennas and a frequency doubler circuit on the same low-cost FR-4 substrate. The fundamental frequency used for the interrogation signal is $f_0=2.5$ GHz, with the second order harmonic $2f_0=5$ GHz generated by the doubler used to send back the information from the tag. Nonlinear simulations based on the NSR201MXT5G diode parameters showed that an input power of only 400 mW at 2.5 GHz is enough to generate a DC current of 2.3 mA and a DC voltage of 4.6 V across a 2kOhm load resistance, and provide an output power of 7.8 mW at 5 GHz. Measurement results demonstrating the energy harvesting feature of the RFID tag show a detected DC current of 0.226 mA at 2.6 GHz for a 300 mm distance between reader and tag antennas for a power of ~ 30 mW (15 dBm) at the reader antenna input. The results show an increase of the readout distance compared to previous work, with a demonstrated RFID link at 100 cm showing a clear rectangular demodulated signal.

Key-words: Energy harvesting; frequency doubler; microstrip patch antenna; RFID; Schottky diode.

1. Introduction

With a 100 years long history [1], the radio frequency identification (RFID) technology has been extensively implemented for tagging, locating, sensing, and tracking objects across a wide range of industries, including retail, logistics, healthcare, automotive and agriculture [2–5].

RFID systems typically consist of two main components: a reader (interrogator) and a tag (transponder). The tag is attached to or embedded in an object, while the reader is used to communicate with the tag wirelessly: the reader transmits an interrogating RF signal towards the tag

that responds with a unique identification signal that is processed by the reader. Traditional RFID tags operate at one fundamental frequency, which is determined by the design and specifications of the RFID system (Fig. 1a). In the case of passive RFID systems, the communication is mainly based on backscattering of the electromagnetic field and the low-power signal returned by the RFID tag is greatly obscured by unwanted radiation clutter, direct coupling, scattering interference and multipath fading in harsh environments. One approach to solving this issue exploits the characteristics of electromagnetic waves polarization diversity, by switching the polarity of the wave reflected by the tag in relation to the incident wave [6–7]. Another solution is to separate the transmit and receive frequencies of the transponder (tag) using frequency conversion [8]. In harmonic systems, the transponder converts the continuous wave interrogating signal at the fundamental frequency f_0 to its second harmonic $2f_0$ (Fig. 1b). This signal is then reflected back and it is detected by a receiver tuned to $2f_0$. The harmonic generation is performed with a non-linear component, generally a low-barrier Schottky diode, and the circuit is called frequency doubler. Harmonic RFID technology represents a powerful and versatile tool for detecting objects in cluttered and noisy environments with an increased read-out distance, which is not possible with conventional RFID systems [9–11].

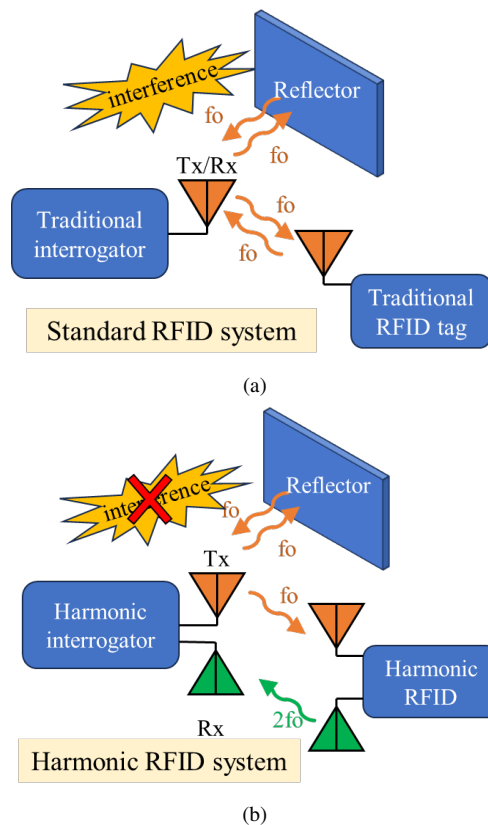


Fig. 1. Block diagram for the RFID system: (a) traditional approach; (b) harmonic generation approach.

The autonomous operation of sensors and low-power electronic devices requires a sustainable energy source that is not based on chemical batteries, which can be difficult to replace in the case of a wireless sensor network located in remote or hard-to-reach locations (underground, areas affected by disasters, agricultural or forest areas, chemical plants) [12–13].

Among other existing energy sources in the environment (sun, wind, vibrations, etc.), the *radio frequency* (RF) electromagnetic fields from cellular telephone networks, telecommunications transmitters, WiFi router signals, radio and TV networks, etc. can penetrate walls and various obstacles and can be a valuable alternative. In the case of a RFID system the RF field energy can be provided by the reader itself and after harvesting it can power sensors and low-power electronic devices adding new functionalities to the RFID tags.

In a harmonic transponder the input power is converted in part to a signal at double the input fundamental frequency and in part to DC power, so this concept is convergent with several new ideas such as *RF energy harvesting* (EH) [14], *RF carrier reuse* [15] and *wireless power transfer* (WPT) [16–17]. This allows for batteryless self-powered and autonomous RFID systems capable of long-term operation without the need for periodic maintenance.

The first steps in the development of such a transponder were reported in [8] and consist of the design, fabrication and measurement of the main circuit blocks: two microstrip antennas operating at 2.5 GHz and 5 GHz and a frequency doubler based on a Schottky diode with input and output transmission line networks placed between the diode and the SMA connectors. The transponder was assembled using coaxial cables and the experimental results validated the concept of harmonic tag.

This paper presents the design, fabrication and measurements of a passive harmonic RFID tag operating with an interrogation signal in the 2.5 GHz frequency range. The microstrip antennas and the frequency doubler are hybrid integrated with Surface Mounted Devices (SMD) on the same *Printed Circuit Board* (PCB) with 105×52 mm overall dimensions (Fig. 2). Microstrip patch antennas are designed for operating frequencies in the 2.5 GHz and 5 GHz frequencies ranges and are measured for input matching and radiation gain extraction. The frequency doubler circuit is design using the small signal bias dependent S parameters for the Schottky diode and 3D electromagnetic modeling. Nonlinear simulations are involved in the calculation of the second order harmonic output power and the harvested DC power. The integrated RFID transponder is fabricated and the experimental results are compared with the simulated ones.

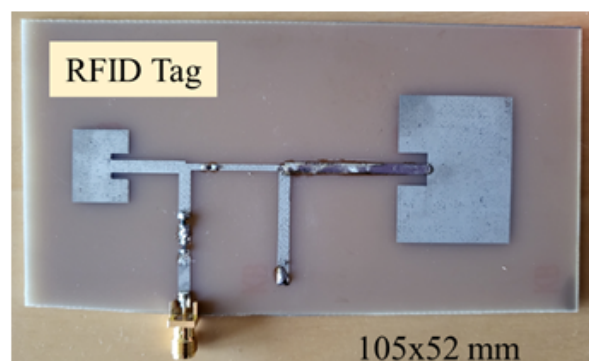


Fig. 2. The fabricated passive harmonic RFID transponder with frequency doubler and energy harvesting features.

2. Circuit Blocks Design and Characterization

A prototype of the proposed harmonic RFID transponder circuit was fabricated using a standard photolithographic process and wet etching of a FR-4 double clad substrate. Both sides of the dielectric substrate were laminated with 35-micron copper sheets and covered with a positive photoresist layer. The mask layout for the frontside metal patterning was transferred using a standard laser printer on a flexible transparent plastic layer which was then placed in direct contact with the photoresist and exposed to UV light. The photoresist was then developed and the copper etched in a ferric chloride solution. The dielectric FR-4 substrate is an epoxy resin substrate reinforced with glass fiber weaving with good RF properties up to several GHz. Its electrical properties vary slightly based on manufacturer but are generally within the 3.8–4.8 range for the relative permittivity and 0.02–0.03 for the loss tangent around 1 GHz. The thickness chosen for this work was 1.54 mm. For this particular FR-4 substrate we measured a relative permittivity of 4.6.

2.1. The microstrip patch antennas optimized for 2.5 GHz and 5 GHz operation

Two microstrip rectangular patch antennas were integrated with the RFID transponder in a planar microstrip configuration. The 3D layout of the antennas was simulated in CST Microwave Studio and designed for the two operating frequencies, 2.5 GHz and 5 GHz. Using the general design rules [18–19], the antenna layouts were optimized using parametric simulations and the final geometrical dimensions in mm for 2.5 GHz (5 GHz) are: patch length $L = 27.4$ (13.4); patch width $W = 35.3$ (17.4); inset length $S = 7$ (4.2) [8]. Antenna samples were fabricated and measured using an Anritsu MS46122A *Vector Network Analyzer* (VNA) and SMA connectors in the experimental setup presented in Fig. 3a). The measured results for the S11 parameter are compared with the simulated results in Fig. 3b). For the two versions, the measured operating frequencies are 2.6 GHz with a 2% fractional bandwidth and 5.2 GHz with 3.4% fractional bandwidth.

Two identical antennas were aligned face-to-face (Fig. 3a)) at a distance of 200 mm and the measured $|S_{21}|$ is shown in Fig. 3c). Using (1), the peak antenna gain was extracted as 7.1 dBi at 2.6 GHz and 8.1 dBi at 5.2 GHz, respectively.

$$\frac{P_r}{P_t} = G_t G_r \left(\frac{\lambda}{4\pi d} \right)^2 \quad (1)$$

where: P_t is the power at the input of the emitting antenna; P_r is the power received by the second antenna; $G_t = G_r$ is the antennas gain; λ is the free space wavelength; d is the distance between the antennas.

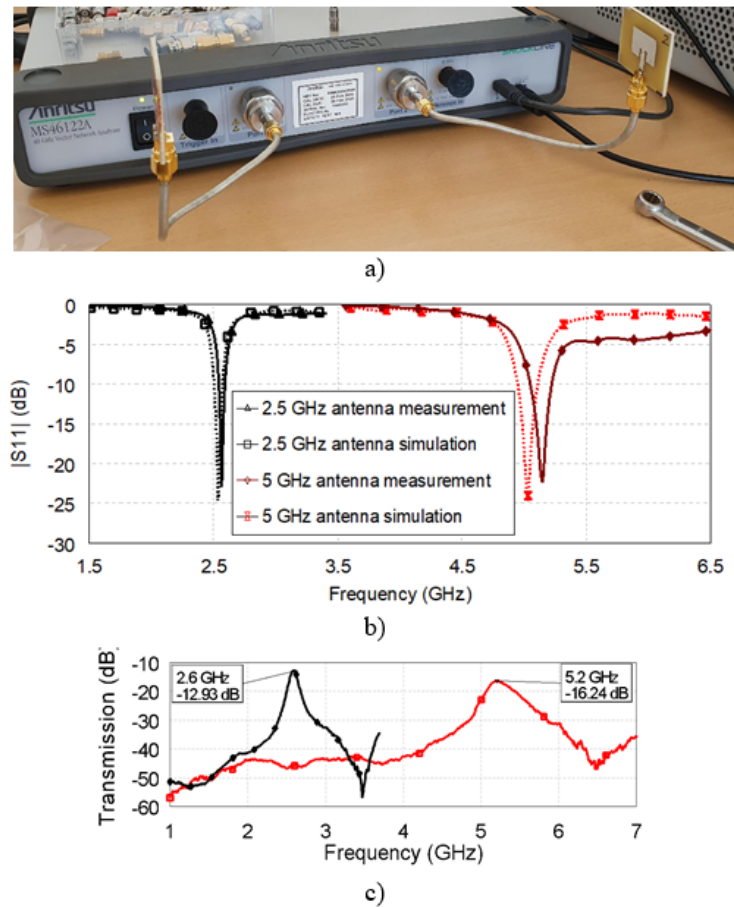


Fig. 3. Antenna measurement: a) the two-antenna measurement setup; b) comparison between simulated and measured S_{11} parameters for the 2.5 GHz (black traces) and 5 GHz (red traces) antennas; c) transmission characteristic as a function of frequency for two identical antennas spaced at 200 mm.

2.2. The microstrip single Schottky diode doubler circuit

A frequency doubler generates an output signal with a frequency which is double that of the input frequency using a nonlinear device. In this work the SMD Schottky diode NSR201MXT5G was used. The diode has an internal zero bias capacitance of 0.15 pF, a series resistance of 14 Ohm and the manufacturer provides the S_{11} reflection parameter in the 1 – 26 GHz frequency range for various bias currents (Fig. 4a)). The measured i/v characteristic is presented in Fig. 4b), and the extracted model parameters are the saturation current $I_S = 156$ nA and ideality coefficient $N = 1.2$.

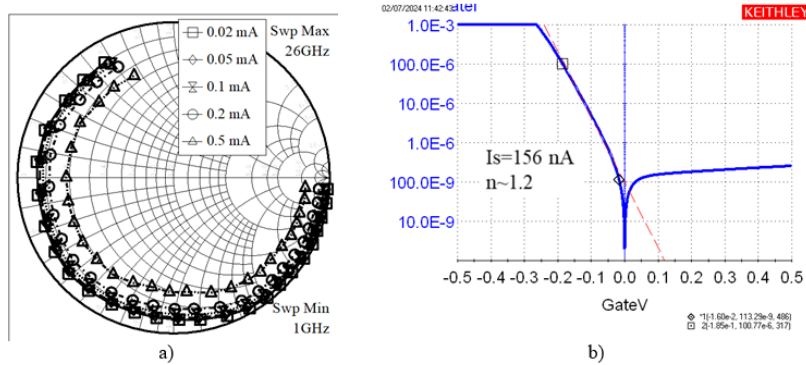


Fig. 4. NSR201MXT5G Schottky diode measurements: a) S11 parameter of the diode as a function of the current; b) measured I/V characteristic of the diode (logarithmic scale).

The circuit design is based on small signal S parameters for a bias current of 0.5 mA and is performed using Cadence AWR *Microwave Office* (MWO). The circuit layout is modeled using the Mentor Graphics SSD (IE3D) software package. Three external ports and one internal port were defined (Fig. 5a)). The circuit model that includes the electromagnetic model (in *.s4p Touchstone format) and diode S parameter block is shown in Fig. 5b).

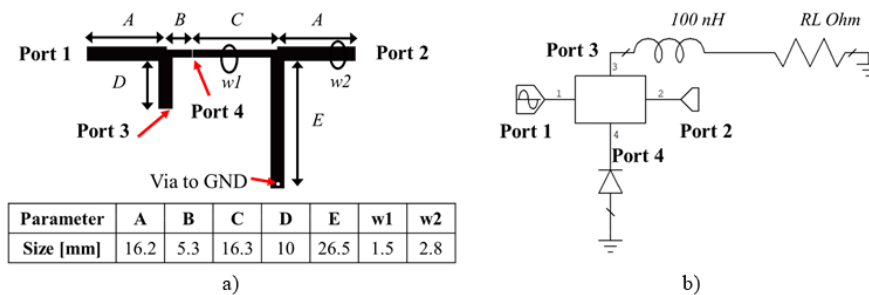


Fig. 5. The frequency doubler circuit: a) electromagnetic model; b) circuit schematic.

The doubler block was fabricated and measured using a VNA. The simulated and measured $|S_{11}|$ (IN at 2.5 GHz) and $|S_{22}|$ (OUT at 5 GHz) were in good agreement and the electromagnetic based modeling approach was validated [8].

For large signal analysis, the built-in nonlinear diode model with the model parameters presented above was connected at port 4 in Fig. 5a). The simulated results for the DC current and the DC voltage across $RL = 2 \text{ k}\Omega$ for an input frequency of 2.5 GHz are presented in Fig. 6. It can be noticed that at an input power of 26 dBm (400 mW) the simulated values of 4.6 V and 2.3 mA are enough to DC bias other electronic circuits needed in a tag for signal processing and provide an output power of 7.8 mW at 5 GHz.

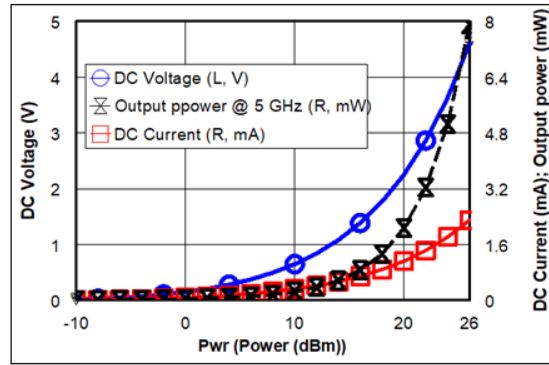


Fig. 6. Simulated results for the DC current and the DC voltage across $R_L = 2$ kOhm for an input frequency of 2.5 GHz.

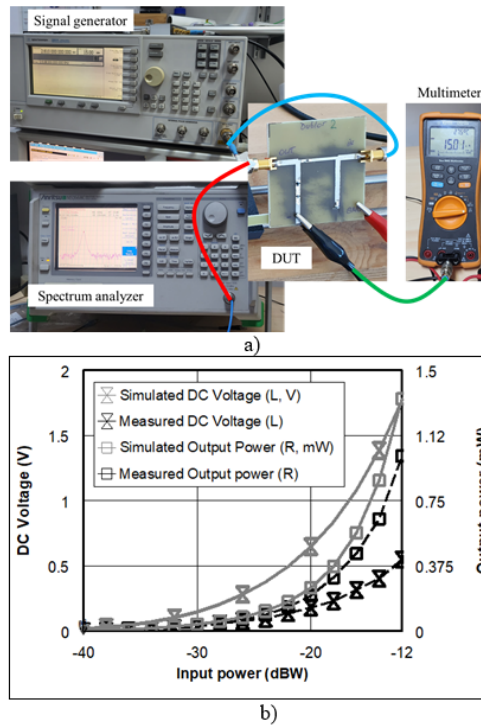


Fig. 7. Nonlinear circuit characterization of the doubler: (a) experimental setup; (b) comparison between nonlinear simulations and measured results for an input frequency of 2.6 GHz.

A diagram of the experimental setup for the nonlinear circuit characterization is presented in Fig. 7a). The *Programmable Signal Generator* (PSG) Agilent is connected at the input of the frequency doubler and the DC current through R_L is measured with a micro-ammeter. The output power is displayed on an Anritsu Spectrum Analyzer. The measured results for an input frequency of 2.6 GHz are compared with nonlinear simulations in Fig. 7b) (the Measured DC

voltage is calculated by multiplying the measured DC current with $R_L = 2 \text{ kohm}$). The input power is varied between $-40 \dots -12 \text{ dBW}$ ($-10 \dots +18 \text{ dBm}$) and the agreement is good for the output power and fairly good for the DC voltage. The differences are due to the limited nonlinear model accuracy.

3. Integrated Harmonic RFID Tag

The photo of the two antennas and the frequency doubler fabricated on the same substrate is shown in Fig. 2. The tag was measured with the experimental setup shown in Fig. 8. For the reader two microstrip patch antennas were fabricated on the same substrate (Fig. 8 – left side). The 2.6 GHz antenna was contacted with a SMA connector and connected with coaxial cables to the PSG, while the 5.2 GHz antenna was connected to the Spectrum Analyzer.

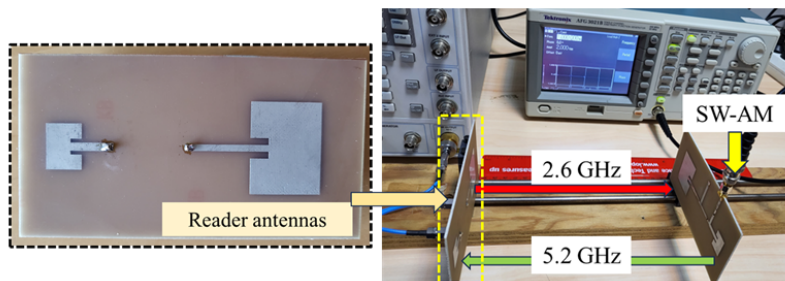


Fig. 8. Experimental setup for the characterization of the integrated RFID tag.

First, the SW-AM SMA port of the tag was connected to a micro-ammeter. The tag was placed at a distance of 300 mm from the reader and the power of the PSG was 15 dBm. The measured DC current is presented in Fig. 9a). The maximum value was 0.226 mA at 2.6 GHz. The circuit model is presented in Fig. 9b) and includes, beside the electromagnetic model and diode model, the measured results for two 2.6 GHz microstrip antennas placed face-to-face at a distance of 300 nm (SUBCKT). The measured and simulated DC current levels are in good agreement even though there is a frequency shift due to modeling parameters accuracy.

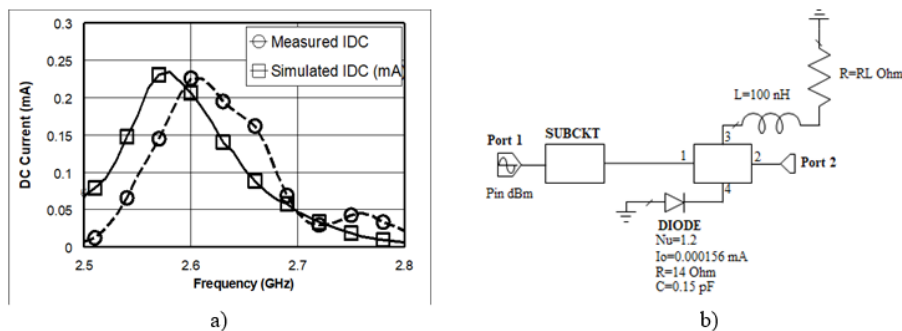


Fig. 9. Energy harvesting using the RFID tag: a) Measured and simulated DC current through R_L as a function of frequency; b) circuit schematic for the simulation of the detected DC current.

Next, the proof of concept was demonstrated, as illustrated in Fig. 8. The tag was illuminated with a 2.6 GHz signal emitted by the reader antenna (input power 15 dBm). A function generator was connected at the SW-AM SMA port of the RFID tag and supplied a square wave voltage between 0V and -2 V (level that switches the diode in its OFF state). In this way, the generated 5.2 GHz output signal is *amplitude modulated* (AM) with a modulation depth of 100% and modulation frequency of 1 kHz.

The signal emitted by the tag is received by the 5.2 GHz reader antenna and plotted on the Spectrum Analyzer using the time domain display function. For an interrogation distance of 100 cm (Fig. 10a)), the received signal is presented in Fig. 10b). In [8], the system was tested for a distance of 10 cm between the reader and tag antennas, resulting in a received power of -46 dBm at 5.2 GHz (reader output power 15 dBm at 2.6 GHz). The increase of the distance to 100 cm will add 40 dB propagation losses lowering the received power to -86 dBm. With the current integrated tag approach, the measured received power level is -73 dBm at a distance of 100 cm. This indicates a remarkable increase in performance (about 13 dB) and thus in the readout range compared to the individual component approach presented in [8].

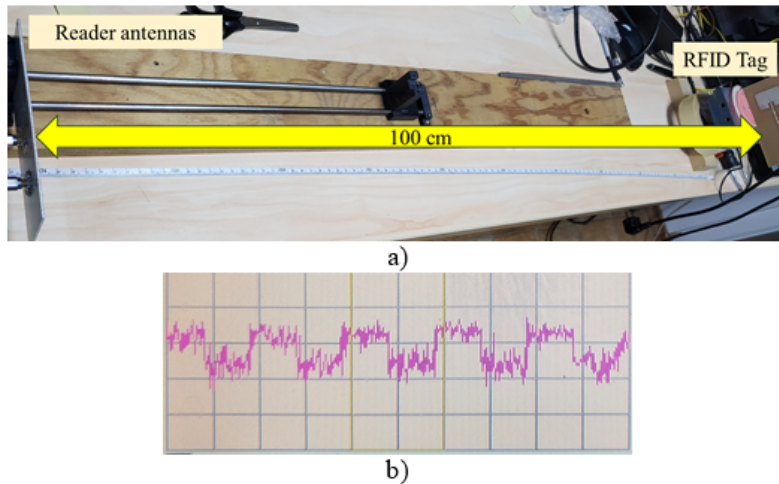


Fig. 10. Proof of concept for a 100 cm distance between the reader and the tag: (a) measurement setup; (b) time domain plot of the signal emitted by the tag and received by the reader at 5.2 GHz.

4. Conclusions

The passive harmonic tag proposed in this paper takes advantage of the nonlinear characteristic of the Schottky diode, adding energy harvesting features to the backscattering of the second harmonic in the RF identification system. The concept was previously demonstrated but the integration of the component blocks of the RFID tag on the same substrate leads to a significant increase of 13 dB of system performance and extends the readout range. Experimental results for a distance of 100 cm between reader and tag show a received power level of -73 dBm for a reader output power 15 dBm at 2.6 GHz and a clearly discernable demodulated rectangular signal at 1 kHz in the raw data. This increase in readout range, as well as the relatively reduced

size of (105×52 mm), low manufacturing costs and batteryless operation feature, recommend it for limited accessibility applications across various industry areas. The 2.5 GHz range interrogation frequency facilitates the future integration with common wireless communication systems operating in the sub-6 GHz bands of 5G/6G and Internet of Things technologies.

Acknowledgements. This work was supported by the Romanian Ministry of Research and Innovation and Digitization, through “ μ NanoEI”, core program project no. 2307/PN23070101, and through “MicroNEx”, Contract nr. 20 PFE /30.12.2021, financed by the Ministry of Research, Innovation and Digitization through Program 1–Development of the National R&D System, Sub-program 1.2–Institutional Performance–Projects for Institutional Excellence.

References

- [1] E. BRARD, *Process for radiotelegraphic or radiotelephonic communication*, Patent US1744036A, 1930.
- [2] A. ABDELNOUR, A. LAZARO, R. VILLARINO, D. KADDOUR, S. TEDJINI and D. GIRBAU, *Passive harmonic RFID system for buried assets localization*, *Sensors* **18**(11), 2018, article number 3635.
- [3] A. SUBRAHMANNIAN and S. K. BEHERA, *Chipless RFID: A unique technology for mankind*, *IEEE Journal of Radio Frequency Identification* **6**, 2022, pp. 151–163.
- [4] G. ANDÍA, Y. DUROC and S. TEDJINI, *Non-linearities in Passive RFID Systems*, J. Wiley & Sons, Hoboken, NJ, 2018.
- [5] N. C. KARMAKAR, E. M. AMINAND and J. K. SAHA, *Chipless RFID Sensors*, J. Wiley & Sons, Hoboken, NJ, 2016.
- [6] D. NECULOIU and A. C. BUNEA, *RFID tag with electromagnetic wave polarization diversity*, *Proceedings of 2021 IEEE International Semiconductor Conference*, Sinaia, Romania, 2021, pp. 1–4.
- [7] D. NECULOIU, A. C. BUNEA and O. G. PROFIRESCU, *Compact implementation of an RFID tag with electromagnetic wave polarization diversity*, *Romanian Journal of Information Science and Technology* **25**(2), 2022, pp. 170–178.
- [8] A. C. BUNEA, O. G. PROFIRESCU and D. NECULOIU, *Passive harmonic RFID tag with energy harvesting features*, *Proceedings of 2023 International Semiconductor Conference*, Sinaia, Romania, 2023, pp. 57–60.
- [9] X. GU, W. LIN, S. HEMOUR and K. WU, *Readout distance enhancement of battery-free harmonic transponder*, *IEEE Transactions on Microwave Theory and Techniques* **69**(7), 2021, pp. 3413–3424.
- [10] M. POLIVKA, V. HUBATA-VACEK and M. SVANDA, *Harmonic balance/full-wave analysis of wearable harmonic transponder for IoT applications*, *IEEE Transactions on Antennas and Propagation* **70**(2), 2021, pp. 977–987.
- [11] T. M. SILVEIRA, P. PINHO and N. B. CARVALHO, *Harmonic RFID temperature sensor design for harsh environments*, *IEEE Microwave and Wireless Components Letters* **32**(10), 2022, pp. 1239–1242.
- [12] M. A. ULLAH, R. KESHAVARZ, M. ABOLHASAN, J. LIPMAN, K. P. ESSELLE and N. SHARIATI, *A review on antenna technologies for ambient RF energy harvesting and wireless power transfer: designs, challenges and applications*, *IEEE Access* **10**, 2022, pp. 17231–17267.
- [13] N. SHINOHARA, *Trends in wireless power transfer: WPT technology for energy harvesting, millimeter-wave/THz rectennas, MIMO-WPT, and advances in near-field WPT applications*, *IEEE Microwave Magazine* **22**(1), 2021, pp. 46–59.

- [14] K. NIOTAKI, N. BORGES CARVALHO, A. GEORGIADIS, X.-Q. GU, S. HEMOUR, K. WU, D. MATOS, D. BELO, R. PEREIRA, R. FIGUEIREDO, H. CHAVES, B. MENDES, R. CORREIA, A. OLIVEIRA, V. PALAZZI, F. ALIMENTI, P. MEZZANOTTE, L. ROSELLI, F. BENASSI, A. COSTANZO, D. MASOTTI, G. PAOLINI, A. EID, J. HESTER, M. M. TENTZERIS and N. SHINOHARA, *RF energy harvesting and wireless power transfer for energy autonomous wireless devices and RFIDs*, IEEE Journal of Microwaves **3**(2), 2023, pp. 763–782.
- [15] X. GU, P. BURASA, S. HEMOUR and K. WU, *Recycling ambient RF energy: far-field wireless power transfer and harmonic backscattering*, IEEE Microwave Magazine **22**(9), 2021, pp. 60–78.
- [16] D. ALLANE, G. ANDIA VERA, Y. DUROC, R. TOUHAMI and S. TEDJINI, *Harmonic power harvesting system for passive RFID sensor tags*, IEEE Transactions on Microwave Theory and Techniques **64**(7), 2016, pp. 2347–2356.
- [17] T. -H. LIN, J. BITO, J. G. D. HESTER, J. KIMIONIS, R. A. BAHR and M. M. TENTZERIS, *On-body long-range wireless backscattering sensing system using inkjet-/3-D-printed flexible ambient RF energy harvesters capable of simultaneous DC and harmonics generation*, IEEE Transactions on Microwave Theory and Techniques **65**(12), 2017, pp. 5389–5400.
- [18] A. PANDEY, *Practical Microstrip and Printed Antenna Design*, Artech House, Boston, MA, London, 2019.
- [19] S. C. BERA, *Microwave Active Devices and Circuits for Communications*, Springer Singapore, Singapore, 2019.